Tracking the built status of MEP works: Assessing the value of a Scan-vs-BIM system

Frédéric Bosché[a], Adrien Guillemet[b], Yelda Turkan[c*], Carl T. Haas[a], Ralph G. Haas[a]

[a]*School of the Built Environment, Heriot-Watt University, Edinburgh, Scotland*

[b]*Department of Civil and Environmental Engineering, University of Waterloo, Ontario, Canada*

[c]*Department of Civil, Construction and Environmental Engineering, Iowa State University, Ames, IA, United States*

Abstract:

Mechanical, Electrical and Plumbing (MEP) works constitute a large portion of construction costs and thus need to be appropriately tracked. Assessment of the built status of MEP works in construction projects is however typically limited to subcontractor claims augmented and contrasted with periodic manual inspection. More detailed manual inspection is costly and not considered worthwhile on most projects. Within a Scan-vs-BIM object recognition framework, three dimensional laser scanning and project 3D/4D BIM models jointly offer the opportunity for frequent, detailed and semantically rich assessment of as built status of construction projects at a cost that continues to decline. This potential has already been demonstrated for tracking structural works, but remains to be assessed in regard to other work sections, in particular MEP works. This paper explores that opportunity. A Scan-vs-BIM processing system is described with some enhancements over previous works. It is then tested with a representative and challenging case study of the construction of a utility corridor in a university engineering building. The results indicate that the proposed system is significantly challenged when tracking MEP systems constructed using traditional on-site fabrication, due to changes or adjustments made on-site that lead to actual component layouts varying in comparison to designed layouts. This performance could be revisited in cases where off-site pre-fabrication and pre-assembly is implemented. The results nonetheless lead the authors to propose a novel data processing system (conceptually described in this paper) integrating Scan-vs-BIM and Scan-to-BIM approaches. This system should provide superior performance over existing systems, enabling automated and robust quality control (including the estimation of the emerging performance metric “percent built as designed”) and delivery of true as-built BIM models to facility owners and managers.

Keywords: MEP works, Scan-vs-BIM, 3D, laser scanning, BIM, as-built status, percent built as designed, Scan-to-BIM

* Corresponding author. Tel.: +1 515 294 7539; fax: +1 515 294 3845. *E-mail addresses:* f.n.bosche@hw.ac.uk (F. Bosché), aguillem@uwaterloo.ca (A. Guillemet), yturkan@iastate.edu (Y. Turkan), chaas@civmail.uwaterloo.ca (C.T. Haas), haas@engmail.uwaterloo.ca (R. Haas)

1 Introduction

1.1 Tracking Progress in the AEC/FM Industry

Progress tracking is traditionally only mentioned with words such as "visual inspections" and "reports". Inspectors are selected and trained to ensure that work meets contract schedule and specifications. Checklists are developed and distributed to inspectors so that they do not overlook critical items. A log is at their disposal to report any deficiency that is then discussed during the weekly meeting [1]. Monitoring progress (including quality) is an extensive manual operation that requires intense labor relying on personal judgment with a high probability of incomplete and inaccurate reports. In the early 2000's, the Architectural Engineering Construction / Facility Management (AEC/FM) industry recognized the urgent need for quick and accurate project progress assessment; the way of monitoring progress had to be reinvented and automated.

In recent years, many researchers came to realize the potential of several new technologies designed in the mid 1990's for automated monitoring. Among those technologies are: Radio Frequency Identification (RFID), Global Positioning System (GPS), Ultra-Wide Band (UWB), Photogrammetry, and Three-dimensional Laser Scanning. For example, Grau et al. [2] examined the productivity impact of automating the identification and localization of engineered components on industrial sites. They quantified and assessed the impact of the automated tracking methodology, a unique combination of RFID, GPS and localization algorithms by considering the traditional tracking process as the baseline for comparison. They concluded that materials tracking technologies can significantly improve craft labor productivity. Ergen et al. [3][4] utilized RFID technology in order to improve facility management processes by locating and tracking facility components automatically. Razavi and Haas [5] deployed a unique combination of GPS, RFID and hand held computing technologies to track key construction materials. The impact on project control and productivity has proven to be substantial. RFID-based indoor location sensing solutions are also investigated by several researchers [6][7][8]. Feasibility of employing UWB technology as a data collection for automated workforce, equipment and material positioning and tracking is investigated by Teizer et al. [9]. Cheng et al. [10] evaluated performance of UWB technology for construction resource location tracking in harsh environments. Shahi et al. [11] presented the performance analysis of an UWB positioning system as a material and activity tracking tool for indoor construction projects. Using statistical analysis, they produced confidence intervals for UWB system error in various tested configurations. Saidi et al. [12] evaluated the static and dynamic performance of a commercially-available ultra-wideband (UWB) tracking system under realistic construction environments for locating and monitoring resources (e.g., people, equipment, and materials). The results and experiences they reported are particularly useful for researchers or practitioners in need of adapting UWB technology for their application.

Golparvar-Fard et al. [13][14] proposed an image-based method for progress monitoring using daily photographs taken from a construction site. In this research, they calibrate (using internal and external calibrations) series of images of the site, and subsequently reconstruct a sparse three-dimensional (3D) as-built point cloud of that site. This allows them to automatically compare as-built data with 3D designed data, and monitor progress. As detailed below, similar approaches have also been proposed using three-dimensional laser scanning, demonstrating significant potential for automated as-built 3D modeling and project monitoring [33][34][38].

The research works above based on RFID, UWB and GPS technology aim at tracking different resources – in particular engineering MEP components – in the supply chain. In comparison, works of Golparvar-Fard et al. [13][14] with photogrammetry or Bosché et al. with laser scanning [33][34] focus on the installation stage and can be used for assessing the quality of that installation. These latter approaches hold much promise for automated progress tracking, but have reported results on structural works tracking only. The work presented here investigates whether the laser-scanning –based approach of Bosché et al. [33][34] performs as well with MEP works as it does for structural works.

1.2 Three Dimensional Laser Scanning

Three dimensional laser scanning, also called LADAR (Laser Detection and Ranging), is an imaging technology that has been increasingly used since the 1990's. It provides fast, accurate, comprehensive and detailed 3D data about scanned scenes. 3D laser scanners essentially give a dense 3D point cloud of the visible scene with millimeter to centimeter accuracy. The density is such that a single full spherical scan can contain millions of points, i.e. with angular resolutions better than 0.01 degrees. The acquired 3D point clouds can be considered as an end product or be used for further purposes such as the creation of as-built 3D (CAD) models for application in design or renovation projects, progress tracking and quality control, for instance.

Laser scanning has been considered by many as the best available technology to capture 3D information on a project with accuracy and speed, with a wide range of applications in the AEC/FM industry [15][16][17][18]. For example, laser scanning has been shown to be valuable to construction managers for progress monitoring, quality control and facility/infrastructure management [19][20][21]. It offers additional value to managers by enabling remote exploration of construction sites and supporting contractor coordination [14]. With respect to quality control in particular, Huber et al. [17] investigated the applicability of laser scanning for analyzing surface flatness, floor plan modeling and recognition of building components. Lijing and Zhengpeng [22] show that the technology offers an advantage over traditional methods of surveying which overlook minor local deformations. Measurement of deterioration for infrastructure is also being investigated for tunnels [20][21], bridges [23][24], and freeways [25]. All these examples illustrate the large range of applications of laser scanning technology today, and explain why the market for laser scanning hardware and software has grown exponentially in the last decade [26]. Much of this growth is now focusing on the interface between scanned data and Building Information Modeling (BIM).

1.3 Laser Scanning and BIM

One of the main applications of laser scanning today is the reconstruction of as-built 3D BIM models from acquired 3D point clouds; a process commonly called *Scan-to-BIM*. There is a significant amount of effort currently being put (both by academia and by private software companies) into developing efficient Scan-to-BIM solutions that are as robust and automated as possible. A review of techniques for automated reconstruction of as-built 3D (BIM) models from laser-scanned point clouds up to 2009 can be found in [27]. That review further refers to the review of free-form object representation and recognition techniques by Campbell and Flynn [28], as well as the more recent review of 3D shape recognition techniques by Shilane et al. [29]. Since 2009 (i.e. the review in [27]), further developments have been made with new approaches for automated pipeline extraction from point clouds [30], as well as automated reconstruction of building indoors (floors, ceilings, walls and windows) [31][32][43]. The *ClearEdge* software suite probably constitutes the state-of-the-art in commercial solution for automated extraction of pipes, in particular.

The rapid development of 3D modeling and BIM offers further perspectives beyond Scan-to-BIM applications. In particular, by aligning laser scans of construction sites with design 3D BIM models and comparing both on the basis of proximity metrics, 3D model objects can be automatically recognized, and very importantly uniquely identified. The authors refer to this process as *Scan-vs-BIM* (as an analogy to *Scan-to-BIM*). A few research teams have already demonstrated the potential value of Scan-vs-BIM processes for tracking progress and dimension quality control of structural works [35][36][37][38]. Similar approaches are also investigated using 3D point clouds generated through photogrammetry instead of laser scanning [13][14].

There is a clear distinction between object recognition approaches typically employed to solve Scan-to-BIM –type problems and Scan-vs-BIM ones. The former can lead to an object being recognized multiple times in a given scene (e.g. pipes with identical dimensions and appearance are recognized as being different occurrences of the same object); while the latter further enable their *identification* because each recognized object refers to a single object within the 3D BIM model. This clear identification constitutes an important strength of Scan-vs-BIM processes – although, as will be shown in this paper, they also present specific limitations.

1.4 Contribution

As discussed above, several research teams have already demonstrated the potential of *Scan-vs-BIM* frameworks for progress tracking. However, these works have so far focused solely on structural components such as floors, ceilings, walls, beams and columns. The research presented here focuses on other important building components, namely mechanical elements such as ducts and pipes. Mechanical, Electrical and Plumbing (MEP) systems constitute a large portion of construction costs and asset value, and thus also need to be appropriately tracked and managed. Knowledge of their as-built status is critical for control and earned value measurement. However, tracking MEP components presents specific and critical challenges compared to structural works. First, MEP components may come in packed configurations that increase the risk of occlusions and more generally of recognition and identification errors (i.e. confusions). Then, their installation in practice, in particular pipes and ducts, seems much more flexible with respect to the positioning of individual components and routes (in comparison with structural components). As a result, the main aim of the research presented here was to assess through a challenging case study the effectiveness of a Scan-vs-BIM system to control MEP works. The results show that, although the proposed Scan-vs-BIM approach demonstrates some advantages and robustness, its performance remains significantly challenged by the variability in MEP component installation. We thus make an additional contribution with the presentation (conceptual) of a novel data processing system that leverages the strengths of Scan-to-BIM and Scan-vs-BIM techniques within a unified framework that has the potential to address their respective limitations. The application of this system is not confined to MEP, but includes essentially any type of works.

2 Three dimensional (3D) Object Recognition Approach

In this section, we summarize the *Scan-vs-BIM* object recognition system (with recent improvements) employed in this research and how it is used to recognize progress of mechanical pipe and ductwork installation works. The approach is based on the comparison of the as-built state captured in the form of three dimensional (3D) point clouds with the expected state defined by the project 3D BIM model [33][34]. Using a 4D BIM model, i.e. by linking an installation schedule to the 3D model, the system can be enhanced to track the actual rate of installation and compare it to the expected one [35][36].

The first (and critical) step of the approach consists in aligning the 3D point clouds in the same coordinate system as the 3D model. This process, commonly called *registration*, should be performed using project survey points. If the building structure has already been controlled dimensionally, then structural elements may be used as alternative survey landmarks, using methods like the one proposed in [40]. Once registration is completed for all available scans, as-built objects can be recognized in the combined point clouds. The recognition algorithm has four steps:

1. *Matching/Recognized Point Clouds:* for each scan, each point is matched to a 3D model object (or none). This leads to an as-built point cloud associated to each 3D model object.
2. *Occluding Point Clouds:* for each scan, the points not matched to any model object but that were acquired from objects lying between the scanner and 3D model objects are identified as occluders.
3. *As-planned Point Clouds:* for each scan, a corresponding (virtual) as-planned scan is calculated using the same scanning parameters. This leads to an as-planned point cloud associated to each 3D model object.
4. *Object Recognition:* for each object, the associated as-planned, as-built and occluding point clouds from all scans are aggregated and jointly analyzed to infer the recognition of the object.

Sections 2.1 to 2.4 review each of these steps, with more details also available in [33][34]. A theoretical assessment of the performance of the proposed method is then made in Section 2.5, prior to the experimental assessment reported in Section 3.

2.1 Recognized Point Clouds

Each point of each registered scan is projected orthogonally on the surfaces of all N_{Obj} objects composing the project 3D model, so that the closest surface matching the point is identified. The following criteria are used: if (1) the distance to that surface, δ_i, is lower than a threshold δ_{max}, and (2) the difference between the normal vectors of the nearby surface and of the point, α, is lower than a threshold α_{max}, then the point is considered *recognized* or *matched* to the corresponding object. We typically use δ_{max}=*30mm* and α_{max}=*45°*.

The result of this process is a segmentation of each initial scan into (N_{Obj} *+ 1)* point clouds; one per object (that includes all the points matched to that object) as well as a one containing all the points not matched to any model object. We call the latter the "NonModel" point cloud. It typically contains points acquired from temporary structures, construction equipment, tools and materials, people, etc. But, as will be discussed later, it may also contain data from project elements whose as-built position and shape differs significantly from their designed ones.

2.2 Occluding Point Clouds

For each as-built scan, the NonModel point cloud is further processed to identify the NonModel points that lay between the scanner and 3D (BIM) model objects. These points are considered to be *occluding* points. The result of this process is not only an overall occlusion point cloud, but also its segmentation into N_{Obj} point clouds; one per 3D model object. Identifying and characterizing occluding point clouds is critical to robust object recognition, as discussed in Section 2.4.

2.3 As-Planned Point Clouds

The next step consists in computing, for each of the input as-built scans, a corresponding (*virtual) as-planned scan*. This is done using the 3D model and the same scanner location and scan resolution. Each as-planned point is calculated by projecting a scanning ray on the 3D model. The result of this process is not only an as-planned scan, but also its segmentation into N_{Obj} point clouds; one per object (that includes all the points that projected onto that object). Note that any ray that doesn't intersect any model object is discarded; i.e. we do not retain any NonModel as-planned point cloud.

2.4 Object Recognition

The recognized, occlusion, non-model and as-planned point clouds from all scans are then aggregated. Each model object then has:

- A *matched (or recognized) point cloud* containing all the scanned points from all scans matched to that object.
- An *occlusion point cloud* containing all the points occluding that object.
- An *as-planned point cloud* containing all the as-planned points matched to that object.

These different point clouds are jointly used to infer the recognition of each model object. For the purpose of robustness to varying scanner-object distances and scan resolutions, recognition is not performed based on the size of the point clouds, but on the surface areas that they cover (see [34] for details). The result is for each model object:

- A *recognized surface* $S_{recognized}$ summing the surface areas covered by all the matched/recognized cloud points:

  $$S_{recognized} = \sum_{i=1}^{n} S_i \qquad (1)$$

  where n is the number of points matched to the object and S_i is the surface covered by the i^{th} matched point.

- An *occlusion surface* $S_{occluded}$ summing the surface areas covered by all the occlusion cloud points (calculated similarly to $S_{recognized}$).
- An *as-planned surface* $S_{planned}$ summing the surface areas covered by all the as-planned cloud points (calculated similarly to $S_{recognized}$).

These different surface areas are finally used to infer the recognition of each model object. For this, we propose the following rule:

> ***If*** ($S_{recognized} \geq S_{min}$ ***or*** $\%_{recognized} \geq \%_{min}^{r}$),
> ***then*** the object is considered recognized;
> ***else*** the object is not recognized.

In the rule above, we use S_{min}= $500cm^2$ that is large enough to ensure that there is sufficient support from the data to infer recognition (in the experiment reported below, $500cm^2$ corresponds approximately to the surface covered by 800 points at 5m from the scanner). However, this high value will prevent the recognition of objects whose recognizable surface ($S_{planned}$ - $S_{occluded}$) is already smaller than S_{min}. To address these cases, the second criterion is used with:

$$\%_{recognized} = \frac{S_{recognized}}{S_{recognizable}} = \frac{S_{recognized}}{S_{planned} - S_{occluded}} \qquad (2)$$

In Equation (2), $S_{planned}$ - $S_{occluded}$ estimates the surface of the object that is theoretically visible, and consequently *recognizable*, from the scanner's location. As a result, $\%_{recognized}$ estimates the percentage of recognizable surface that is recognized. In the recognition rule above, we use $\%^{r}_{min} = 50\%$.

While the rule above provides a binary decision on the recognition of object, it can be noted that a low value of $\%_{recognized}$ also indicates that fewer points than expected are recognized. Therefore, $\%_{recognized}$ could be used to assess the *level of confidence* with which objects are recognized. However, $\%_{recognized}$ depends on the number of matched points (or more exactly their covered surface), but doesn't really take into account the deviations between these points and the surfaces they are matched to. In other words, $\%_{recognized}$ does not fully take account of the deviations that may be observed between the as-built and designed positions of objects. To address this, we propose the following metric to assess the level of confidence, $\%_{confidence}$:

$$\%_{confidence} = \frac{S^{w}_{recognized}}{S_{recognizable}} = \frac{S^{w}_{recognized}}{S_{planned} - S_{occluded}} \qquad (3)$$

where $S^{w}_{recognized} = \sum_{i=1}^{n} \left(1 - \left|\frac{\delta_i}{\delta_{max}}\right|^2\right) S_i$

with n, S_i, δ_i, δ_{max} as previously defined.

Compared to $S_{recognized}$ (Equation (1)), $S^{w}_{recognized}$ is the weighted sum of the surfaces covered by the points matched to each object, where higher weights are given to points that are closer to the object. $\%_{confidence}$ *thus* extends $\%_{recognized}$ by taking account for the deviation between the as-built and designed positions of objects.

Note that the proposed point and object recognition metrics as well as recognition confidence level constitute additions to and improvements of the approach previously published by the authors in [33] and [34].

2.5 Theoretical performance analysis

In this section, we conduct a theoretical performance analysis of the proposed Scan-vs-BIM recognition process for MEP works, focusing on the risk of false negatives, false positives as well as confusions:

False Negatives (objects present but not recognized): The recognition rule has been designed to be robust with regard to the recognition of objects that are small or that are highly occluded. Nonetheless, the value of δ_{max} constrains the amount of deviations between the actual and design position (both location and orientation) of objects that the system can handle. As discussed earlier, MEP elements may present deviations much larger than structural elements, which may show the limit of the proposed approach for tracking MEP works.

False Positives (objects recognized but not present): The chosen value of S_{min} may first seem to be not sufficiently large to avoid false positives. However, we remind that S_{min} is the surface covered by scan points matched to the object and that this matching requires closeness both in distance and surface normal orientation. The combination of these two rules reduces the risk that points be matched to the wrong object, and therefore the risk of false positives. Furthermore, in the experiment reported below, 500cm^2 corresponds approximately to the surface covered by 800 points at 5m from the scanner, which is a fairly large number of points. A false positive could thus only occur when an object has been positioned on site in a way that part of its surface is at a location and with an orientation close to those designed for a 3D model object. Nonetheless, we will show that the recognition confidence level $\%_{recognized}$ provides valuable information that can be leveraged to prevent such errors.

Confusions: An important situation when a false negative and a false positive can jointly occur is when a model object has an actual position that significantly deviates from its design position (false negative) but this actual position is such that its surface matches the design position of the surface of another model object (false positive). Such a situation results in what is called a *confusion*, and the current system is theoretically unable to address such challenging cases, although, as discussed above, the recognition metrics are designed to reduce the risk of false positives.

3 Experiments

An experiment has been conducted using real life data to evaluate the performance of the proposed approach for tracking MEP works.

3.1 Data

The data collected include 2D CAD drawings and frequent laser scans of the Engineering VI Building at the University of Waterloo, a five-storey, 100,000-square-foot building that is designed to shelter the Chemical Engineering Department of the university. A 3D CAD model was then created by the authors following accurately the information provided in the 2D drawings.

The project was a perfect fit for this study, since a chemical facility like the Engineering VI Building provides a large number of pipes and ducts designed to: (1) provide water and gas to different laboratories, and (2) collect and evacuate chemical fumes from them. The attention of this study was focused on the service corridor of the fifth floor of the building because of the abundance of pipes coming from the lower levels and going all the way up to the penthouse. The 3D CAD model created from those 2D drawings by our research team is shown in Figure 1.

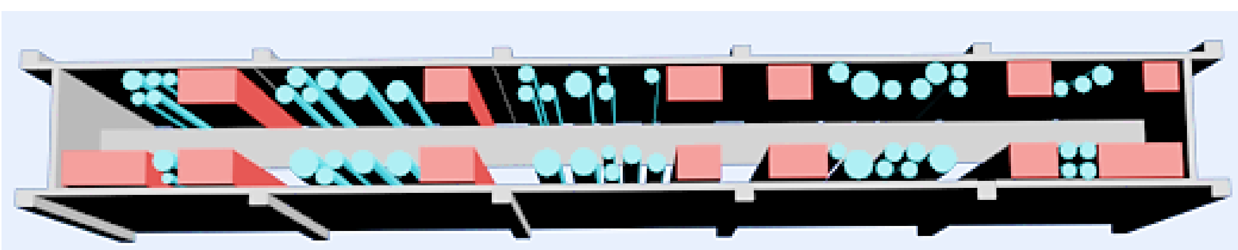

Figure 1: 3D model of the 5th floor corridor Engineering VI.

The laser scanner used in this study is a FARO Laser Scanner LS 880 HE. The scanner implements phase based technology, and its main technical characteristics are given in Table 1 [41]. The service corridor of the 5th floor of the building, with dimensions 31.0m x 3.4m, was scanned from June 2010 to February 2011, but the experimental results presented in this paper were obtained using only the scans acquired on February 5th 2011 because they contain data from a larger number of pipes and ducts. Due to the narrowness of the corridor and density of pipes and ducts, six scans were acquired along the corridor (see Figure 2). Each scan contains about 1,000,000 points, with horizontal and vertical resolutions of 2200μrad and 4400μrad respectively (i.e. 0.24° x 0.48°). Registration of the scans with the

3D model was achieved using the approach described in [40], using the wall, floor and ceiling planes as registration landmarks. Accurate registration was achieved for each scan, with an average of around 30,000 scan points matched to the planes and an average mean square error of 58mm^2. The 3D model and integrated point cloud illustrate the relative density of pipes and ducts as well as the limited access that led to a fair amount of occlusions.

Table 1: Characteristics of the FARO LS 880 HE scanner

Laser Type:	785nm; near infrared
Distance: Range:	0.6 m to 76m.
Accuracy:	± 3 mm @ 25 m.
Angle: Range:	Hor: 360°; Vert: 320°
Max. Resolution:	Hor: 13 µrad; Vert: 157 µrad
Acquisition Speed:	up to 120,000 pts/s

(a)

(b)

Figure 2: Ensemble of point-clouds acquired on the 5th floor service corridor of the E6 Building. (a): top view of the registered point clouds with the location of the six scans shown in red; (b): view of inside the corridor from one of the scanning locations.

3.2 Recognition Results

Figure 3 shows the portion of the 2D drawing presenting a top view of the mechanical pipes and ducts in the investigated corridor. The figure highlights the result of a manual identification in the scans of the actual presence of the different mechanical objects. This information is not used by the recognition system; it is solely used as ground truth for the calculation of its performance, as explained later.

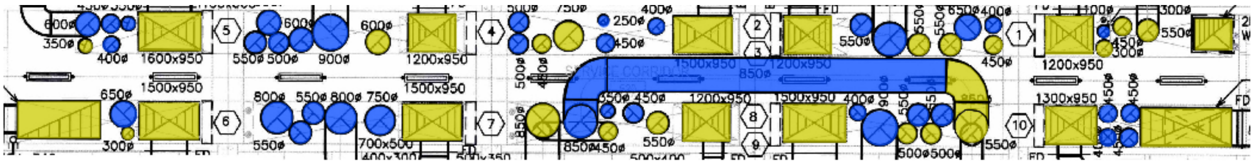

Figure 3: Manual analysis of the presence of mechanical elements in the scans:
***Yellow*: element present; *Blue*: element absent.**

Figure 4 illustrates the object recognition results obtained for *δ_{max}=30mm, α_{max}=45°, S_{min}=500cm^2 and $\%^r_{min}$=50%*. Figure 4(a) highlights which objects are correctly recognized (true positive), incorrectly recognized (false positive), correctly not recognized (true negative) and incorrectly not recognized (false negative). Figure 4(b) further details these results by showing the level of confidence, *$\%_{confidence}$*, for each object. Objects are colored based on *$\%_{confidence}$* and grouped in three categories of level of confidence: High (*50%<$\%_{confidence}$*); Medium-low (*5%<$\%_{confidence}$ <50%*); and Very low (*$\%_{confidence}$ <5%*). These categories were defined ad-hoc and were found to capture the different situations encountered. Table 2 summarizes the results of Figure 4.

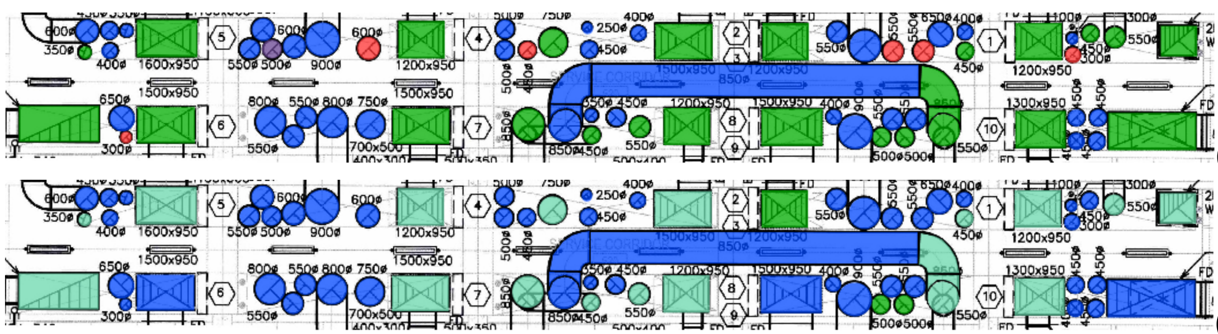

(a)

(b)

Figure 4: Recognition results obtained for *δ_{max}=30mm, α_{max}=45°, S_{min}=500cm^2 and $\%^r_{min}$=50%*:
(a) Recognition decision: *Green*: true positive; *Red*: false negative; *Blue*: true negative; *Magenta*: false positive; (b) Level of confidence: *Green:* high level of conference (*50%<$\%_{confidence}$*); *Turquoise*: medium to low level of confidence (*5%<$\%_{confidence}$ <50%*); *Dark Blue*: very low level of confidence (*$\%_{confidence}$ <5%*).

Table 2: Summary of the recognition and confidence level results shown in Figure 4.

Actual State	Recognized State	Total	$\%_{confidence}$		
			High	Medium -low	Very Low
Present	Present	26	3	19	4

	Absent	6	0	0	6
Absent	Present	1	0	0	1
	Absent	39	0	0	39[a]

[a] *For a large majority of true negatives, $\%_{confidence}$ is actually null.*

3.3 Performance Analysis

Information in the column 'Total' in Table 2 enables the calculation of commonly used recognition performance metrics, namely *Precision* and *Recall*. *Precision* is the percentage of objects recognized that are actually present in the scan(s) (see Equation (4)); and *Recall* is the percentage of objects present in the scan(s) that are actually recognized (see Equation (5)). A high Recall rate indicates that most building 3D elements present in the scans are recognized, hence a good performance with regard to false negatives; a high Precision rate indicates a good performance with regard to false positives.

$$\text{Precision} = \frac{\sum TP}{\sum P} = \frac{\sum TP}{\sum TP + \sum FP} \quad (4)$$

$$\text{Recall} = \frac{\sum TP}{\sum Pr} = \frac{\sum TP}{\sum TP + \sum FN} \quad (5)$$

where *P* = Positive (i.e. recognized), *TP* = True Positive, *FP* = False Positive, *Pr* = Present, and *FN* = False Negative.

Precision and false positives: With a precision of 96% [= 26 / (26 + 1)], it appears that the system performs well with regard to false positives. Although this may be due to the particular context of the experiment, this is also explained by the combination of distance and normal orientation criteria for matching points to model objects that minimizes the likelihood that a point is matched to the wrong object (see example in Figure 5(a)). False positives can thus occur only if an object (contained or not in the 3D model) has a part of its surface that is similarly positioned (both location and orientation) as the surface of another object contained in the 3D model. In the experiment conducted by the authors, one such false positive occurs as illustrated in Figure 5(b) where a small pipe not contained in the 3D model is positioned in a way that the larger one is wrongly recognized. However, as shown in Table 2, the level of confidence in the recognition of that pipe is actually estimated by the system to be very low. This demonstrates the value of the proposed level of confidence metric.

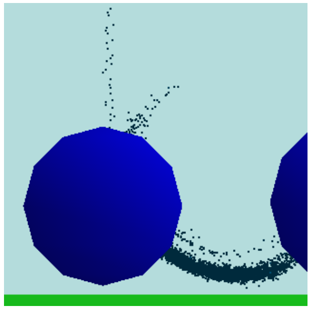
(a)

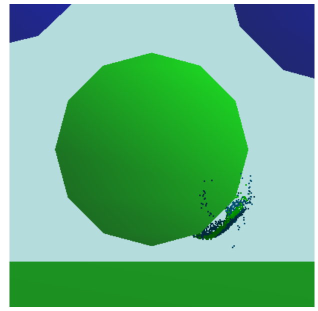
(b)

Figure 5: False positives: (a) Two examples of potential false positives avoided by the system. In both cases, none of the scanned points is matched to any of the two objects (thanks to the surface normal matching criterion); (b) False positive encountered in the reported experiment; a small pipe not contained in the 3D model is positioned in a way that the pipe (green) is wrongly recognized.

Recall and false negatives: With a recall of 81% [= 26 / (26 + 6)], the system appears not to perform well in recognizing installed MEP objects. In fact, this performance is much lower than the one previously reported on tracking structural work, where recall and precision rates both achieved nearly 100% [35][36]. In addition, the levels of confidence reported for MEP elements is generally below 50%, which is also much lower than what the authors have observed for structural elements (e.g. >80% for the walls delimiting the corridor, and similar results with other datasets). The reason for the high rate of false negatives is due to the fact that, as was anticipated, installation of mechanical elements is geometrically less constrained than that of structural elements, so that the actual and designed positions of some mechanical elements may differ. This is what happens for the six false positives reported in Table 2; two of these are illustrated in Figure 6. From this, it is concluded that the proposed approach for object recognition, that has shown very good performance for tracking structural works, is not adequate for tracking MEP works (at least when traditional fabrication methods are used, as discussed later in Section 5.2).

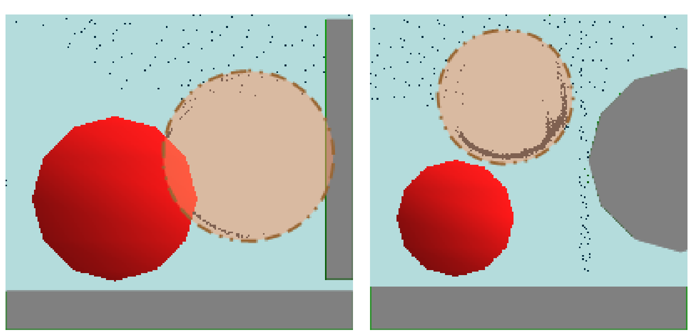

Figure 6: Two of the six false negatives. The objects are shown in red at their designed location, and in transparent orange at their actual one (in the point cloud).

Level of confidence $\%_{confidence}$: Table 2 indicates that true positives present a wide range of value for $\%_{confidence}$. This actually confirms the presence of deviations between the as-built and designed positions of MEP elements. As shown in Figure 7, there is indeed a good correlation between values of $\%_{confidence}$ and the level of these deviations. It must be noted that in one occasion, a very low level of $\%_{confidence}$ is observed that is not just due to position deviation, but actually due to the object (a duct) having an as-built shape different from its designed one.

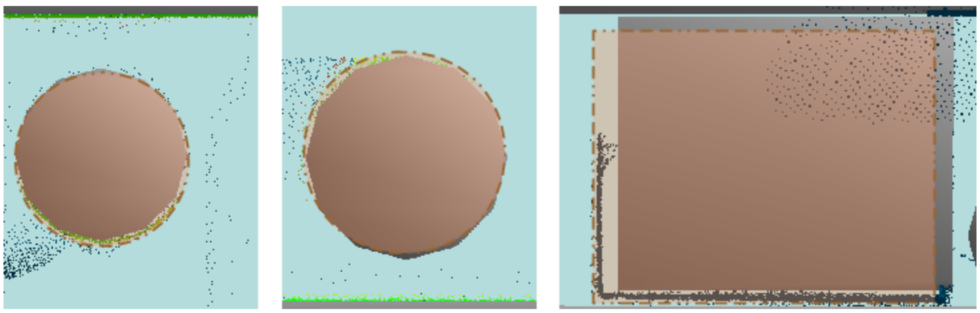

(a) Elements recognized with *high* level of confidence.

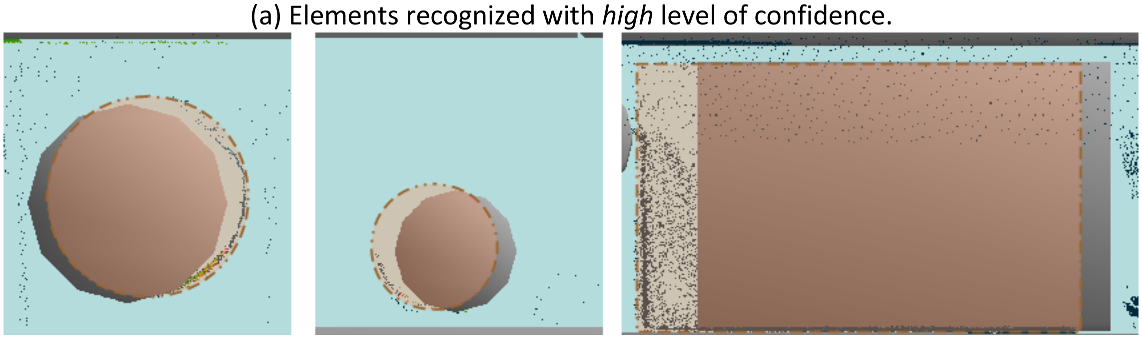

(b) Elements recognized with *medium* level of confidence.

Figure 7: Correlation between level of confidence and deviation between as-built and designed locations for recognized objects. Objects are shown in gray at their designed location, and in transparent orange at their actual one (in the point cloud).

In summary, while the proposed Scan-vs-BIM system does not perform well in recognizing all objects in a scene, it is however able to recognize objects *built as-planned*, given pre-defined tolerances. Thus, by specifying tolerances for point deviation (i.e δ_{max}) and overall object deviation (e.g. $\%^{c}_{min}$ to threshold $\%_{confidence}$), the proposed system can automatically recognize all objects built within those tolerances. This has two important potential applications:

1. **Dimensional quality control**: *"Percent built as designed"* is a term that is emerging in practice [42]. Although the authors have not identified a clear definition of it, in essence it aims at integrating progress and quality performance, by quantifying the overall deviation between the designed state – e.g. as defined in the 3D (BIM) model – and as-built state of

projects. Using the proposed system with defined tolerances, an estimate of "*percent built as designed"* with focus on geometry/dimensions could be obtained automatically.

2. **Delivery of true as-built 3D (BIM) models**: As reported in the literature review, academia and industry are currently putting significant efforts into developing robust and efficient Scan-to-BIM algorithms, supporting the reconstruction of true as-built BIM models from laser scanning data. These approaches systematically aim at re-modeling entire facilities from scratch, in order to address the most general cases where no prior information is available. However, in the case of projects (new builds or renovations) for which 3D BIM is used during design (slowly becoming standard practice), the prior information contained in the 3D BIM model can be leveraged. Using the proposed Scan-vs-BIM system with specified tolerances, objects that are within tolerances with regard to their designed shape and position can be automatically identified. These objects would not need to be remodeled, so their designed position and shape can be considered adequate for re-use in the as-built 3D model. Engineers would then only need to focus their attention on re-modeling those objects with deviations beyond tolerances. This *filtering* functionality could save significant amounts of time in preparing true as-built 3D models to be delivered to clients. This idea is considered as part of a new data processing system that is introduced later in Section 4.

3.4 Sensitivity Analysis

The proposed system requires a certain number of parameters to be defined including: δ_{max}, α_{max}, S_{min}, $\%^{r}_{min}$, and eventually $\%^{c}_{min}$. We focus our attention on two parameters that are likely to impact the performance reported earlier: δ_{max} and S_{min}. As a sensitivity analysis, the experiments below show the impact of different values of δ_{max} and S_{min} on the recognition performance.

$\boldsymbol{\delta_{max}}$: Results obtained for δ_{max}=10mm, δ_{max}=50mm and δ_{max}=70mm are shown in Figure 8, and summarized in Table 3 along with those obtained for δ_{max}=30mm (all other parameters remaining unchanged). As expected, the recall and level of confidence increase with δ_{max}, but this increase is more significant from 10mm to 30mm than from 30mm to 70mm. Regarding false positives, precision is not significantly impacted although an additional false positive occurs for δ_{max}=50mm and a third one occurs for δ_{max}=70mm. Although this should be confirmed by further experiments, these results indicate that δ_{max} should probably be set between 30mm and 50mm. Below 30mm, the risk of false negatives increases sharply while precision is likely to improve only marginally; above 50mm, the risk of false positive increases while recall will likely increase only marginally.

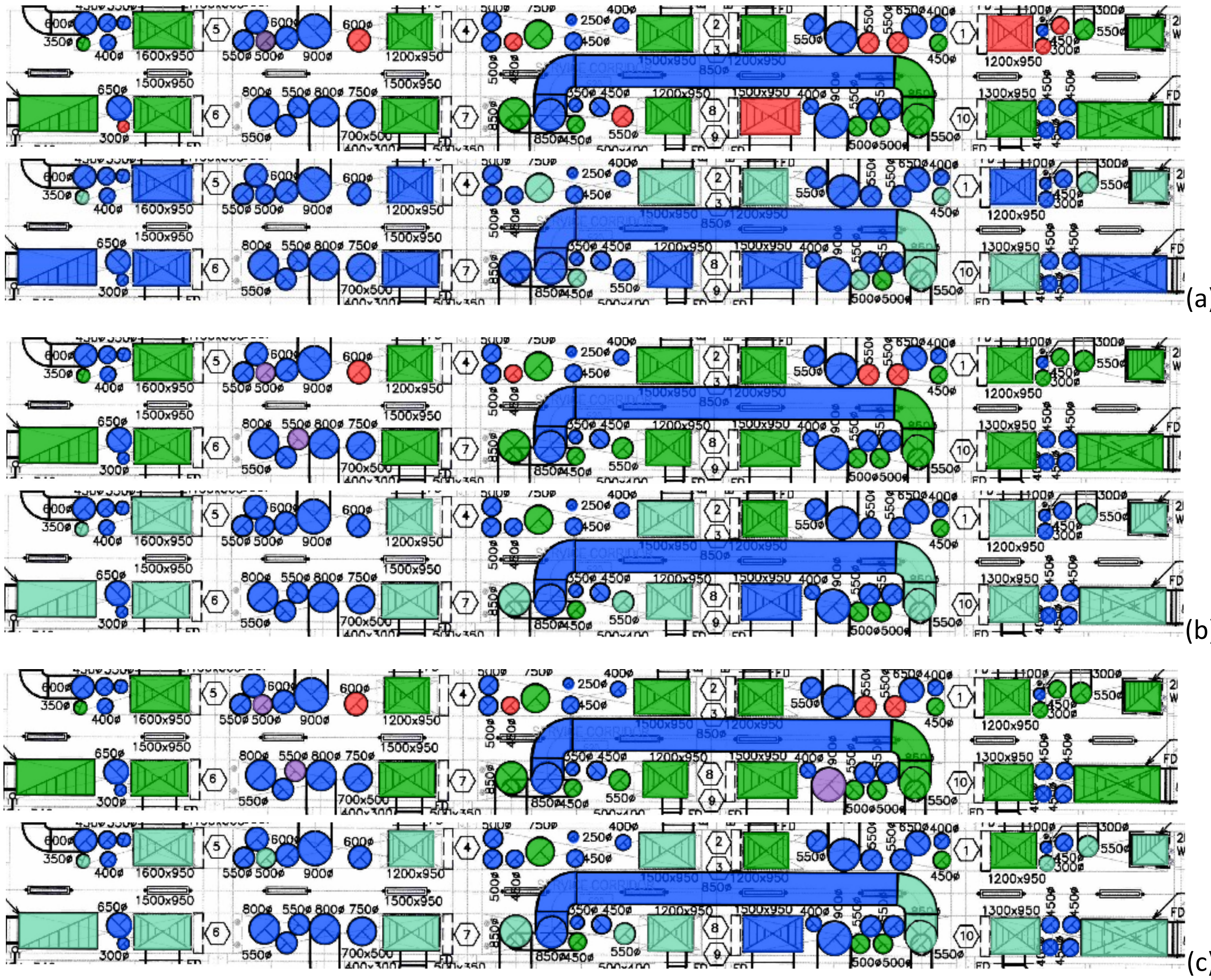

Figure 8: Recognition results for δ_{max}=10mm (a), δ_{max}=50mm (b) and δ_{max}=70mm (c). The same color-coding as in Figure 4 is used.

Table 3: Summary of the recognition results for δ_{max}=10mm, δ_{max}=50mm and δ_{max}=70mm (Figure 8) as well as δ_{max}=30mm (Figure 4 and Table 2).

δ_{max} (mm)	Actual State	Recognized State	Total	%*confidence*		
				High	Medium -low	Very low
10.0	Present	Present	22	1	13	8
		Absent	10	0	0	7
	Absent	Present	1	0	0	1
		Absent	39	0	0	39[a]

30.0	Present	Present	26	3	19	4
		Absent	6	0	0	6
	Absent	Present	1	0	0	1
		Absent	39	0	0	39[a]
50.0	Present	Present	27	6	18	3
		Absent	4	0	0	4
	Absent	Present	2	0	0	2
		Absent	38	0	0	38[a]
70.0	Present	Present	27	7	18	2
		Absent	4	0	0	4
	Absent	Present	3	0	1	2
		Absent	37	0	0	37[a]

[a] *For a large majority of true negatives, $\%_{confidence}$ is actually null.*

S_{min}: Results obtained for S_{min}=*100cm*^{2} and S_{min}=*1000cm*^{2} are shown in Figure 9, and summarized in Table 4 along with those previously obtained for S_{min}=*500cm*^{2} (all other parameters remain as initially defined). Note that $\%_{confidence}$ is independent of S_{min}, and so is not analyzed here. As expected, the recall decreases as S_{min} increases. But, this decrease is more significant from 500cm^2 to 1000cm^2. Regarding false positives, precision seems to be rapidly impacted for values of S_{min} below 500cm^2. As a result, although this should also be confirmed by further experiments, these results indicate that a value of S_{min} around 500cm^2 seems appropriate to optimize the quality of the results.

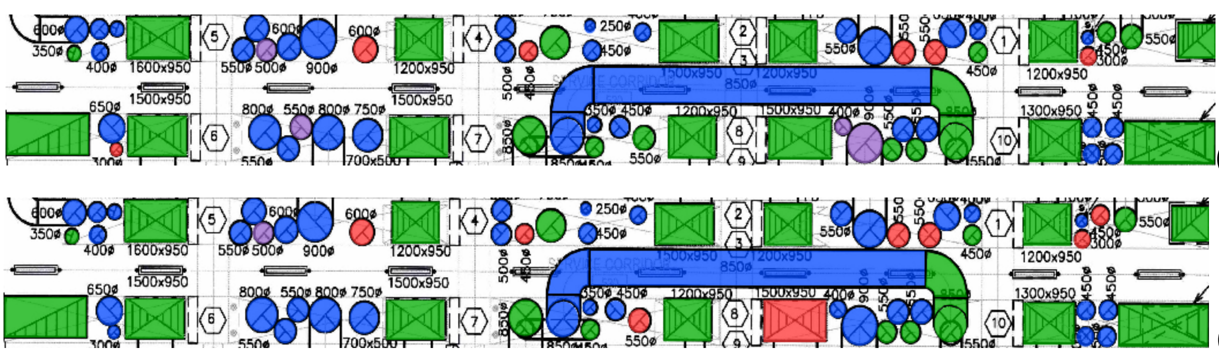

(a)

(b)

Figure 9: Recognition results for S_{min}=100cm^2 (a) and S_{min}=1000cm^2 (b)
The same color-coding as in Figure 4 is used.

Table 4: Summary of the recognition results for S_{min}=100cm^{2}mm and S_{min}=1000cm^2 (Figure 9) as well as S_{min}=500cm^2 (Figure 4 and Table 2).

S_{min} (cm^2)	Actual State	Recognized State	Total

100	Present	Present	26
		Absent	6
	Absent	Present	4
		Absent	36
500	Present	Present	26
		Absent	6
	Absent	Present	1
		Absent	39
1000	Present	Present	23
		Absent	8
	Absent	Present	1
		Absent	39

4 Improved Data Processing System

Although the proposed Scan-vs-BIM approach demonstrates some advantages and robustness, the results reported here highlight that the good performance achieved with structural works is far from being achievable with MEP works. This is due to the flexibility and resulting variability in MEP component installation.

We note that the common Scan-to-BIM -type object recognition methods reviewed in Section 1 (as reviewed in [27][28][29]) actually show complementary strengths and limitations. Indeed, while unable to provide a direct identification of objects, they are however insensitive to the actual locations of objects within the scene (the main limitation of our approach).

This leads the authors to propose a system that integrates Scan-to-BIM and Scan-vs-BIM techniques within a unified framework that leverages the strengths of both approaches. The system does not focus on any type of works (e.g. MEP), but is aimed to be a system for *life-cycle BIM model dimensional information management*. It would thus support activities such as progress control, dimensional quality control and subsequently efficient delivery of dimensionally-correct as-built BIM models during construction; and later on dimensional monitoring during the Operations and Maintenance (O&M) phase of the asset life.

The proposed BIM model dimensional information management system, illustrated in Figure 10, processes 3D point clouds (from laser scanning or photogrammetry) – possibly augmented with additional sensed data such as RFID (the potential of using RFID with laser scanning is shown in [43]), UWB or digital pictures – of the structure in its current state (*as-built* during construction; *as-is* during operations). The overall system is composed of three consecutive processes:

1. *An automated object recognition process* employing techniques currently considered in Scan-to-BIM processes for *recognizing* objects of interest (with basic or complex geometries) in the sensed data. This process is *supervised*, driven by prior geometric and semantic (including topology) information about the objects being searched; this prior information comes from the most current BIM model (*as-designed* during construction; *as-built* and *as-is* later on during operations) and may be completed with other information about additional objects that may be expected.

   In more detail, this process would first extract primitive geometries (e.g. planes) and their configuration (i.e. topology) [44][27]. This information would then be analyzed using the prior information on surface patch geometry and topology contained and extracted from the BIM model. This latter step differs from the approach proposed in [44][27], mainly because they assume a context without prior BIM models. The output of this process is a list of recognized objects with their configuration and associated levels of confidences.

2. *An automated Scan-vs-BIM process* that employs the recognition results of step 1 and further prior information contained in the most current BIM model, e.g. expected object location and orientation; model topology , in an object *identification* process based on the one proposed in this paper. The output of this process is a list of identified objects with associated levels of confidences, as well as information on deviations between the as-built [current as-is] and as-designed [previous as-is] BIM models. These deviations may be displacements and deformations, or unidentified objects.

3. *A semi-automated BIM Model Correction process* for correcting any identified deviations using automated, semi-automated, and manual workflows and thus updating the BIM model to a new most current as-built [as-is] state.

While the system altogether enables the management of a dimensionally correct as-built [as-is] 3D BIM model during its entire life-cycle, steps 1 and 2 may also be used alone during the construction phase for dimensional quality control and quality assessment (including for estimating of the "percent built as planned" metric presented earlier).

Furthermore, it is important to point out that most of, if not all, the different approaches reviewed in Section 1 (with focus on Scan-to-BIM or Scan-vs-BIM) could be integrated within the first or second step of this new system.

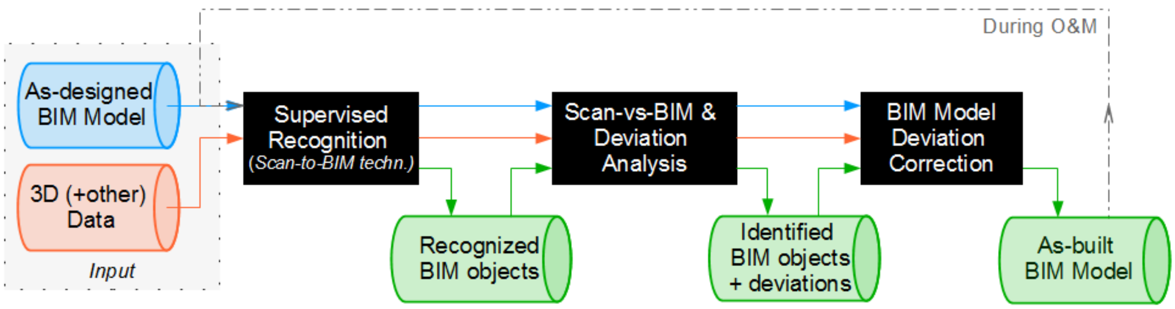

Figure 10: Proposed data processing system for life-cycle BIM model dimensional information management.

Taking the example of pipework, step 1 enables the recognition of objects such as pipes (cylinders), elbows (torus) and valves (complex objects). Step 2 then enables their identification by matching them with individual components contained in the BIM model, using a combination of physical and appearance proximity metrics. Compared to the current system, this new step 2 ensures that the points matched to a cylindrical pipe themselves form a cylinder, further ensuring the level of confidence in the recognition. Step 3 finally enables the correction of deviations observed for these objects.

This overall process should be initiated during the construction stage in order to control dimensional quality and produce a dimensionally correct 3D BIM model, and continued during O&M in order to update the model over time and maintain a history of deviations that could support maintenance decision making processes.

Zeibak-Shini [45] have recently proposed a framework for reconstruction of as-is BIM models of deformed structures in post-disaster building assessment using TLS data and a prior BIM model, which is very similar to the one proposed here. Like in our approach, they propose to use surface primitives, their configuration and prior information contained in the BIM model in order to recognize as-built objects. The main difference seems to be on the reconstruction of the as-built BIM model; while they seem to simply recognize (actually identify) objects based on matched surface patches and retrieve their as-built shape from the TLS data only, the approach proposed here differently aims to “deform” the prior BIM model in order to make it fit the as-built data. Interesting, they refer to their last step as “BIM-to-BIM”, a term that would actually (better) suit the third step of the approach proposed here.

5 Conclusion and Future Work

5.1 Conclusion

Most of the research effort on automated construction progress tracking has focused so far on structural work. However, other building components, and in particular MEP systems, constitute a large portion of construction costs and thus need to be appropriately tracked and managed. Knowledge of their as-built status is critical for control and earned value measurement. The work presented here constitutes one of the few reported attempts to address this problem, and is unique in assessing a Scan-vs-BIM framework for such application.

An experiment using data from a utility corridor containing a few dozens of pipes and ducts is reported. While results are reported for this case study only, it must be emphasized that it is representative of situations typically encountered.

The results with regard to object recognition, and consequently the potential for progress tracking, are however disappointing. The authors were conscious that the installation of MEP pipes and duct in traditional ways is not as constrained as structural works, so that elements may be installed in positions that differ, sometimes significantly, from the positions defined by the engineer in the design drawings/model. The experiments have confirmed that these deviations can significantly impact the performance of the proposed Scan-vs-BIM system that has previously been shown to perform well for tracking structural works.

Beyond demonstrating the limitation of the author’s Scan-vs-BIM approach for tracking construction works, the results reported further suggest (and some voices have started to raise this issue) that clients should not consider as-designed 3D BIM models entirely usable for Operation & Maintenance (O&M) and future refurbishment, as many on-site changes or adjustments may not have been reported in those models.

Nonetheless, other valuable results have emerged from the experiments, particularly with regard to the newly proposed *level of confidence* metric, $\%_{confidence}$. Although this remains to be confirmed with additional experiments, results reported here suggest that $\%_{confidence}$ is a valuable metric to estimate deviations (both minor and major) between the as-built and as-designed position and shape of objects; and this property could make the proposed system valuable for automatically estimating the emerging performance metric "percent built as designed".

5.2 Future Work

The results reported in this paper answer one question, but also raise many new questions that require future investigations. First, future work should thoroughly assess the value of using the proposed Scan-vs-BIM systems for (1) estimating "percent built as designed", and (2) accelerating of as-built modeling.

Then, the authors note that the experiments reported here used data from a project where MEP pipes and ducts were installed using traditional methods (i.e. cut and fit on site). With the advent of BIM and the increasing use of off-site pre-fabrication and pre-assembly, the likelihood that MEP elements are installed in similar positions as designed should significantly increase. The proposed Scan-vs-BIM system may perform much better in such context. This should thus be investigated by acquiring data (laser scans and 3D models) from different projects actively employing pre-fabrication and pre-assembly of MEP systems.

Finally, the authors recognize that the risk of false positives, including confusions, remains significant when using the proposed Scan-vs-BIM; this approach should thus not be used alone, particularly when it comes to MEP works. Further work should thus investigate integrating the proposed system with additional techniques for object recognition. With this in mind, the authors have proposed a new data processing system for 3D BIM model dimensional information management that aims to integrate supervised Scan-to-BIM and Scan-vs-BIM approaches in an overall superior system. Such a system now needs to be developed, and its performance assessed.

6 Acknowledgments

The authors would like to thank Gary Caldwell from Aecon Group Inc. for providing the 2D drawings of Engineering V Building, and for allowing Adrien Guillemet to take the scans of the construction. The authors would also like to thank to Arash Shahi and Yazan Chaban from University of Waterloo for their help during this work.

This research is partially funded by NSERC CRD Grant, NSERC Discovery Grant, CII and SNC Lavalin.

7 References

[1] J.E. Schaufelberger, L. Holm, Management of Construction Projects: A Constructor's Perspective, Prentice Hall (2002).

[2] D. Grau, C.H. Caldas, C.T. Haas, P.M. Goodrum, J. Gong, Assessing the impact of materials tracking technologies on construction craft productivity, Automation in Construction. 18 (2009) pp. 903-911.

[3] E. Ergen, B. Akinci, R. Sacks, Tracking and locating components in a precast storage yard utilizing radio frequency identification technology and GPS, Automation in Construction. 16 (2007), pp. 354-367.

[4] E. Ergen, B. Akinci, R. Sacks, Life-cycle data management of engineered-to-order components using radio frequency identification, *Automation in Construction*, 21 (2007), pp. 356-366.

[5] S.N. Razavi, C.T. Haas, Multisensor data fusion for on-site materials tracking in construction, *Automation in Construction*, 19 (2010), pp. 1037-1046.

[6] N. Li, B. Becerik-Gerber, Performance-based evaluation of RFID-based Indoor Location Sensing Solutions for the Built Environment, *Advanced Engineering Informatics*, 25 (3) (2011), pp. 535–546.

[7] S.N. Razavi, O. Moselhi, GPS-less indoor construction location sensing, *Automation in Construction*, 28 (2012), pp. 128-136.

[8] A. Pradhan, E. Ergen, B. Akinci, Technological Assessment of Radio Frequency Identification Technology for Indoor Localization, ASCE Journal of Computing in Civil Engineering. 23 (4) (2009) pp. 230-238.

[9] J. Teizer, M. Venugopal, A. Walia, Ultrawideband for Automated Real-time Three-Dimensional Location Sensing for Workforce, Equipment, and Material Positioning and Tracking,

Transportation Research Record, Transportation Research Board of the National Academies, Washington D.C (2008), pp. 56–64.

[10]T. Cheng, M. Venugopal, J. Teizer, P.A. Vela, Performance evaluation of ultra-wideband technology for construction resource location tracking in harsh environments, *Automation in Construction*, 20(8) (2011) pp. 1173-1184.

[11]A. Shahi, A. Aryan, J.S. West, C.T. Haas, R.G. Haas, Deterioration of UWB positioning during construction, *Automation in Construction*, 24 (2012), pp. 72-80.

[12]K.S. Saidi, J. Teizer, M. Franaszek, A.M. Lytle, Static and dynamic performance evaluation of a commercially-available ultra wideband tracking system, *Automation in Construction*, 20 (2011) pp. 519-530.

[13]M. Golparvar-Fard, F. Pena-Mora, S. Savarese, Application of D4AR – A 4-Dimensional augmented reality model for automating construction progress monitoring data collection, processing and communication, Journal of Information Technology in Construction. 14 (2009) pp. 129-153.

[14]M. Golparvar-Fard, F. Peña-Mora, S. Savarese, Automated progress monitoring using unordered daily construction photographs and IFC-based Building Information Models, *ASCE Journal of Computing in Civil Engineering*, (2013), in press.

[15]W. Stone, G. Cheok, *LADAR sensing applications for construction*, Building and Fire Research, National Institute of Standards and Technology (NIST), Gaithersburg, MD (2001).

[16]G. Cheok, W. Stone, R. Lipman, C. Witzgall, Ladars for Construction Assessment and Update, *Automation in Construction*, 9 (2000) pp. 463-477.

[17]D. Huber, B. Akinci, P. Tang, A. Adan, B. Okorn, X. Xiong, Using Laser Scanners for Modeling and Analysis in Architecture, Engineering, and Construction, *Proceedings of the 44th Annual Conference on Information Sciences and Systems*, (2010) pp. 1-6.

[18]G. Jacobs, 3D scanning: Using multiple laser scanners on projects, *Professional Surveyor Magazine*, 28 (2008).

[19]F. Bosché, C.T. Haas, Automated retrieval of 3D CAD model objects in construction range images, *Automation in Construction*, 17 (2008), pp. 499-512.

[20]D.W. Qui, J.G. Wu, Terrestrial laser scanning for deformation monitoring of the thermal pipeline traversed subway tunnel engineering, *XXIst ISPRS Congress: Commission V, WG 3*, Beijing, (2008), pp. 491-494.

[21]P. Biddiscombe, 3D Laser scan tunnel inspections keep expressway infrastructure project on schedule, *Trimble^{TM} Navigation White Paper*, (2005).

[22]B. Lijing, Z. Zhengpeng, Application of point clouds from terrestrial 3D laser scanner for deformation measurements, *The International Archives of the Photogrammetry, Remote Sensing and Spatial Information Sciences*, Beijing. 37 (2008), Part B5.

[23]H.S. Park, H.M. Lee, H. Adeli, I. Lee, A new approach for health monitoring of structures: terrestrial laser scanning, *Journal of Computer Aided Civil and Infrastructure Engineering*. 22 (2007), pp. 19-30.

[24]W. Liu, S. Chen, E. Hauser, LiDAR-based bridge structure defect detection, *Experimental Techniques*, 35(6) (2011), pp. 27-34.

[25]K.S. Yen, K. Akin, B. Ravani, Accelerated Project Delivery: Case Studies and Field Use of 3D Terrestrial Laser Scanning in Caltrans Projects, Advanced Highway Maintenance and Construction Technology Research Center, Research Report UCD-ARR-08-06-30-0, (2008).

[26]T. Greaves, B. Jenkins, 3D laser scanning market red hot: 2006 industry revenues 253 million, 43% growth, *SparView*, 5 (2007).

[27]P. Tang, D. Huber, B. Akinci, R. Lipman, A. Lytle, Automatic reconstruction of as-built building information models from laser-scanned point clouds: A review of related techniques, *Automation in Construction*, 19(7) (2010), pp. 829-843.

[28]R. Campbell, P. Flynn, A survey of free-form object representation and recognition techniques, *Computer Vision and Image Understanding (CVIU)*, 81(2) (2001).

[29]P. Shilane, P. Min, M. Kazhdan, et al., The Princeton Shape Benchmark, in *Proceedings of Shape Modeling International*, Genova, Italy (2004).

[30]J. Lee, C. Kim, H. Son, C.-H. Kim, Automated pipeline extraction for modeling from laser scanned data, *International Symposium on Automation and Robotics in Construction (ISARC)*, Eindhoven, the Netherlands, (2012).

[31]E. Valero, A. Adán and C. Cerrada, Automatic Method for Building Indoor Boundary Models from Dense Point Clouds Collected by Laser Scanners, *Sensors*, 12 (2012), pp. 16099-16115.

[32]X. Xiong, A. Adan, B. Akinci, D. Huber, Automatic creation of semantically rich 3D building models from laser scanner data, Automation in Construction, 31 (2013), pp. 325-337.

[33]F. Bosché, C.T. Haas, Automated retrieval of 3D CAD model objects in construction range images, *Automation in Construction*, 17 (2008), pp. 499-512.

[34]F. Bosché, Automated recognition of 3D CAD model objects and calculation of as-built dimensions for dimensional compliance control in construction, Advanced Engineering Informatics. 24 (2009), pp. 107-118.

[35]Y. Turkan, F. Bosché, C.T. Haas, R.G. Haas, Automated progress tracking using 4D schedule and 3D sensing technologies, Automation in Construction. 22 (2012), pp. 414-421.

[36]Y. Turkan, F. Bosché, C.T. Haas, R. Haas, Automated Earned Value Tracking using 3D Imaging Tools, *ASCE Journal of Construction Engineering and Management*, 139 (4) (2013), pp. 423-433 .

[37]P. Tang, E. Anil, B. Akinci, D. Huber, Efficient and Effective Quality Assessment of As-Is Building Information Models and 3D Laser-Scanned Data, *ASCE International Workshop on Computing in Civil Engineering* (2011), Miami, FL.

[38]C. Kim, H. Son, C. Kim, Automated construction progress measurement using a 4D building information model and 3D data, Automation in Construction, 31 (2013), pp. 75-82.

[39]R. Issa, I. Flood, W. O'Brien (ed.), 4D CAD and Visualization in Construction: Developments and Applications, Taylor and Francis (2003).

[40]F. Bosché, Plane-based Coarse Registration of 3D Laser Scans with 4D Models, Advanced Engineering Informatics. 26 (2011), pp. 90-102.

[41]Faro Technologies Inc., *Faro Laser Scanner 880 HE Handbook*, Faro Technologies Inc., Lake Mary, FL, USA (2007).

[42]N. Post, Pioneers push paradigm shift, *Engineering News Record (ENR)*, September 2011

[43]E. Valero, A. Adan, C. Cerrada, Automatic Construction of 3D Basic-Semantic Models of Inhabited Interiors Using Laser Scanners and RFID Sensors, *Sensors*, *12 (*2012), pp. 5705-5724.

[44]X. Xiong, D. Huber, Using Context to Create Semantic 3D Models of Indoor Environments, *Proceedings of the British Machine Vision Conference (BMVC*) (2010), Aberystwyth, UK.

[45]R. Zeibak-Shini, R. Sacks, S. Filin, Toward generation of a Building Information Model of a deformed structure using laser scanning technology, 14th International Conference on Computing in Civil and Building Engineering (ICCCBE) (2012), Moscow, Russia.